51. Neutrino Cross Section Measurements

Revised August 2019 by G.P. Zeller (FNAL).

Neutrino cross sections are an essential ingredient in all neutrino experiments. Interest in neutrino scattering has recently increased due to the need for such information in the interpretation of neutrino oscillation data [1]. Historically, neutrino scattering results on both charged current (CC) and neutral current (NC) channels have been collected over many decades using a variety of targets, analysis techniques, and detector technologies. With the advent of intense neutrino sources constructed for neutrino oscillation investigations, experiments are now remeasuring these cross sections with a renewed appreciation for nuclear effects[1] and the importance of improved neutrino flux estimations. This work summarizes accelerator-based neutrino cross section measurements performed in the $\sim 0.1 - 300$ GeV range with an emphasis on inclusive, quasi-elastic (pionless), and pion production processes, areas where we have the most experimental input at present (Table 51.1). For a more comprehensive discussion of neutrino cross sections, including neutrino-electron elastic scattering and lower energy neutrino measurements, the reader is directed to a review of this subject [2]. Here, we survey existing experimental data on neutrino interactions and do not attempt to provide a census of the associated theoretical calculations [3], which are both critical and plentiful, or the important constraints being gleaned from electron-nucleus scattering as input to neutrino event generators.

Table 51.1: List of beam properties, nuclear targets, and run durations for modern accelerator-based neutrino experiments studying neutrino scattering.

Experiment	beam	$\langle E_\nu \rangle$, $\langle E_{\overline{\nu}} \rangle$ GeV	neutrino target(s)	run period
ArgoNeuT	$\nu, \overline{\nu}$	4.3, 3.6	Ar	2009 – 2010
ICARUS (at CNGS)	ν	20.0	Ar	2010 – 2012
K2K	ν	1.3	CH, H_2O	2003 – 2004
MicroBooNE	ν	0.8	Ar	2015 –
MINERvA	$\nu, \overline{\nu}$	3.5 (LE), 5.5 (ME)	He, C, CH, H_2O, Fe, Pb	2009 – 2019
MiniBooNE	$\nu, \overline{\nu}$	0.8, 0.7	CH_2	2002 – 2019
MINOS	$\nu, \overline{\nu}$	3.5, 6.1	Fe	2004 – 2016
NOMAD	$\nu, \overline{\nu}$	23.4, 19.7	C–based	1995 – 1998
NOvA	$\nu, \overline{\nu}$	2.0, 2.0	CH_2	2010 –
SciBooNE	$\nu, \overline{\nu}$	0.8, 0.7	CH	2007 – 2008
T2K	$\nu, \overline{\nu}$	0.6, 0.6	CH, H_2O, Fe	2010 –

51.1 Inclusive Scattering

Over the years, many experiments have measured the total inclusive charged current cross section for neutrino ($\nu_\mu N \rightarrow \mu^- X$) and antineutrino ($\overline{\nu}_\mu N \rightarrow \mu^+ X$) scattering off nucleons covering a broad range of neutrino energies. As can be seen in Fig. 51.1, the inclusive cross section approaches a linear dependence on neutrino energy. This behavior is expected for point-like scattering of neutrinos from quarks, an assumption which breaks down at lower energies. Modern

---

[1]Nuclear effects refer to kinematic and final state effects which impact neutrino scattering off nuclei. Such effects can be significant and are particularly relevant given that modern neutrino experiments make use of nuclear targets to increase their event yields.

measurements of such inclusive scattering cross sections and their target nuclei are summarized in Table 51.2.
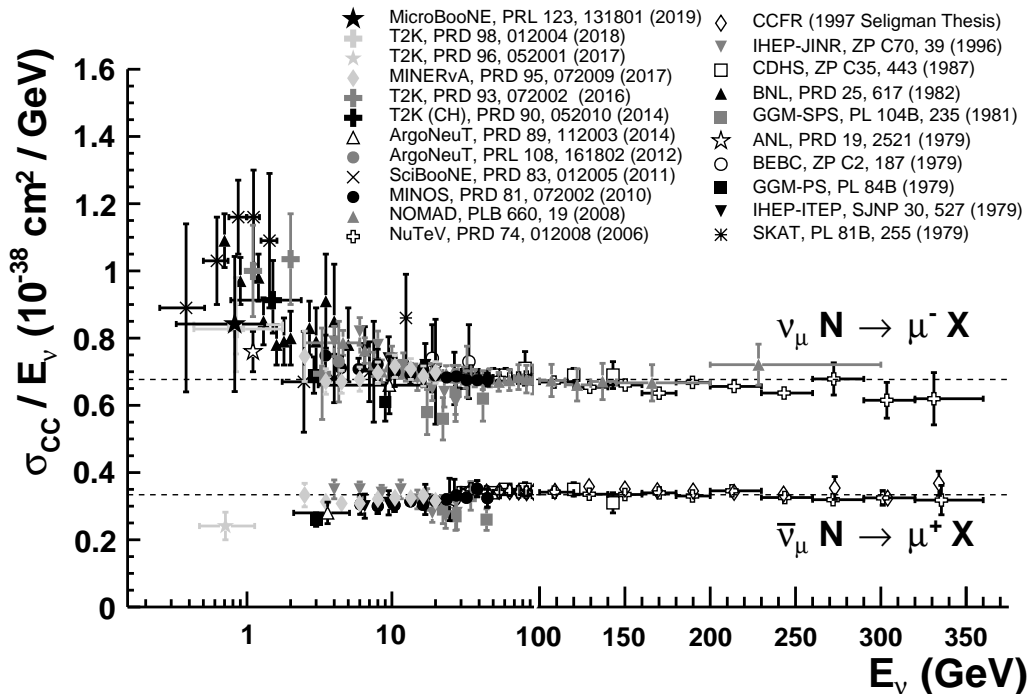

Figure 51.1: Measurements of per nucleon ν_μ and $\overline{\nu}_\mu$ CC inclusive scattering cross sections divided by neutrino energy as a function of neutrino energy. Note the transition between logarithmic and linear scales occurring at 100 GeV. Neutrino cross sections are typically twice as large as their corresponding antineutrino counterparts, although this difference can be larger at lower energies. NC cross sections (not shown) are generally smaller compared to the CC case.

To provide a more complete picture, single and double differential cross sections for such inclusive scattering processes have been reported – these include measurements on iron from NuTeV [4] and, more recently, on a variety of nuclear targets from ArgoNeuT [5,6], MicroBooNE [7], MINERvA [8], and T2K [9,10]. More recently, MicroBooNE has measured the multiplicity of charged tracks emanating from neutrino scattering on argon [11] and T2K has reported detailed ratios of CC cross sections on hydrocarbon, water, and iron [12]. T2K has also provided the first measurement of the antineutrino CC inclusive cross section at low energy [13] (Fig. 51.1). At high energy, the inclusive cross section is dominated by deep inelastic scattering (DIS). Several neutrino experiments have measured DIS cross sections for specific targets and final states, for example, MINERvA has measured ratios of muon neutrino inclusive and DIS cross sections on a variety of nuclear targets including lead, iron, and carbon [14,15]. Other experiments have measured opposite-sign dimuon production, the most recent being from CHORUS [16], NOMAD [17], and NuTeV [18]. At lower neutrino energies, the inclusive cross section is an additionally complex combination of quasi-elastic scattering and pion production processes, two areas we discuss next.

Table 51.2: Published measurements of neutrino and antineutrino CC inclusive cross sections from modern accelerator-based neutrino experiments.

experiment	measurement	target
ArgoNeuT	ν_μ [5,6], $\overline{\nu}_\mu$ [6]	Ar
MicroBooNE	ν_μ [7]	Ar
MINERνA	ν_μ [8,14,15,19], $\overline{\nu}_\mu$ [19], $\overline{\nu}_\mu/\nu_\mu$ [20]	CH, C/CH, Fe/CH, Pb/CH
MINOS	ν_μ [21], $\overline{\nu}_\mu$ [21]	Fe
NOMAD	ν_μ [22]	C
SciBooNE	ν_μ [23]	CH
T2K	ν_μ [9,10,12,24,25], ν_e [26,27], $\overline{\nu}_\mu/\nu_\mu$ [13]	CH, H_2O, Fe

51.2 Quasi-elastic scattering

Quasi-elastic (QE) scattering is the dominant neutrino interaction for neutrino energies less than ~ 1 GeV and represents a large fraction of the signal samples in many neutrino oscillation experiments, which is why this process has received considerable attention in recent years. Historically, neutrino (antineutrino) quasi-elastic scattering refers to the process, $\nu_\mu n \to \mu^- p$ ($\overline{\nu}_\mu p \to \mu^+ n$), where a charged lepton and single nucleon are ejected in the elastic interaction of a neutrino (or antineutrino) with a nucleon in the target material. This is the final state one would strictly observe, for example, in scattering off of a *free* nucleon target. There were many early measurements of neutrino QE scattering that span back to the 1970's [2]. In many of these initial measurements, bubble chamber experiments employed light targets (hydrogen or deuterium) and required both the detection of the final state muon and single nucleon[2]; thus the final state was clear and elastic kinematic conditions could be verified. The situation is more complicated, of course, for heavier nuclear targets used in modern neutrino experiments. In this case, nuclear effects can impact the size and shape of the cross section as well as the final state composition, kinematics, and topology. Due to intranuclear hadron rescattering and the effects of correlations between target nucleons, additional particles may be ejected in the final state; hence, a QE interaction on a nuclear target does not necessarily imply the ejection of a lepton and a *single* nucleon. One therefore needs to take care in defining what one means by neutrino QE scattering when scattering off targets heavier than hydrogen or deuterium. Because of this, modern experiments tend to instead report cross sections for processes involving pionless (e.g., nucleon-only) final states, often referred to as CC 0π or QE-like reactions in recent literature. Such measurements are summarized in Table 51.3. Many modern experiments have also recently opted to report nucleon-only cross sections as a function of final state particle kinematics [28–36]. Such distributions can be more difficult to directly compare between experiments but are much less model-dependent and provide more stringent tests of the theory than historical cross sections as a function of neutrino energy (E_ν) or 4-momentum transfer (Q^2). Recent work has been done to develop a means to directly compare experimental measurements produced in these less model-dependent forms [37].

The topic of neutrino QE scattering began drawing increased attention following the first double differential cross section measurements of this process that revealed a significantly larger cross section than originally anticipated, predominantly in the backwards muon scattering region [31,32]. Such an enhancement was observed many years prior in transverse electron-nucleus scattering [55] and was attributed to the presence of correlations between target nucleons in the nucleus. As a result, the impact of such nuclear effects on neutrino QE scattering has recently become the subject of intense experimental and theoretical scrutiny with implications on event rates, nucleon emission,

---

[2]In the case of deuterium, many experiments additionally observed the spectator proton.

Table 51.3: Published measurements of CC and NC scattering cross sections with nucleon-only final states from modern neutrino experiments.

experiment	measurement	target
ArgoNeuT	2p [38]	Ar
K2K	M_A [39]	H_2O
MINERνA	$\frac{d\sigma}{dQ^2}$ [40–42], 1p [43], ν_e [44], $\frac{d^2\sigma}{dp_T dp_{||}}$ [28,29], $\frac{d\sigma}{dp_n}\frac{d\sigma}{d\delta\alpha_T}$ [30], $\frac{d^2\sigma}{dE_{avail}dq_3}$ [45]	CH, Fe, Pb
MiniBooNE	$\frac{d^2\sigma}{dT_\mu d\theta_\mu}$ [31,32], M_A [46], NC [47,48]	CH_2
MINOS	M_A [49]	Fe
NOMAD	M_A, $\sigma(E_\nu)$ [50]	C
Super-K	NC [51]	H_2O
T2K	$\frac{d^2\sigma}{dT_\mu d\theta_\mu}$ [33–35], $\sigma(E_\nu)$ [52], M_A [53], NC [54], $\frac{d\sigma}{d\delta p_T}\frac{d\sigma}{d\delta\alpha_T}$ [36]	CH, H_2O

neutrino energy reconstruction, and neutrino versus antineutrino cross sections. The reader is referred to reviews of the situation in [3,56,57]. To help drive further progress in understanding the underlying nuclear contributions, pionless (e.g., nucleon-only) cross sections have been reported for the first time in the form of double-differential distributions by MiniBooNE [31,32], MINERvA [28,29,45], and T2K [33–35]. Such double-differential cross sections in terms of final state particle kinematics reduce some of the model-dependence of the reported data, provide the most robust measurements available, and allow a more rigorous two-dimensional test of the underlying nuclear theory. MINERvA and T2K have been especially prolific in recent years in probing this interaction process (Table 51.3). Neutrino experiments have also launched dedicated studies of the hadronic side of these interactions, including ArgoNeuT [38,58], MINERvA [43], and T2K [36]. MINERvA has been the first modern experiment to measure neutron emission in antineutrino interactions [59]. In addition, the exploration of transverse kinematic variables in neutrino scattering is allowing better constraints on the various contributions to the cross section, including recent evaluations from MINERvA [28–30] and T2K [36]. With the MiniBooNE results having first revealed these additional complexities in neutrino-nucleus QE scattering, measurements from multiple neutrino experiments, on other targets, and using additional kinematics are crucial for getting a better handle on the underlying nuclear physics impacting neutrino-nucleus interactions. What we once thought was "simple" QE scattering is in fact not so simple.

In addition to such charged current investigations, measurements of the neutral current counterpart of this channel have also been performed. The most recent NC elastic scattering cross section measurements include those from BNL E734 [60], MiniBooNE [47,48], Super-K [51], and T2K [54]. A number of measurements of the Cabibbo-suppressed antineutrino QE hyperon production cross section have additionally been reported [61,62], although not in recent years.

51.3 Pion Production

In addition to such elastic scattering processes, neutrinos can also inelastically scatter producing a nucleon excited state (Δ, N^*). Such baryonic resonances quickly decay, most often to a nucleon and single-pion final state. Historically, experiments have measured various exclusive final states associated with these reactions, the majority of which have been on hydrogen and deuterium targets [2]. There have been several recent re-analyses of this data to better understand the consistency between data sets [63], nucleon form factors [64], and non-resonant contributions [65]. Also, modern measurements of neutrino-induced pion production have since been performed on a variety of nuclear targets (Table 51.4).

In addition to resonance production processes, neutrinos can also coherently scatter off of the

Table 51.4: Summary of modern measurements of NC and CC scattering cross sections involving a pion (or pions) in the final state.

experiment	$\pi^{\pm}$ measurement	π^0 measurement	target
ArgoNeuT	CC [66]	NC [67]	Ar
K2K	CC [68,69]	CC [70], NC [71]	CH, H_2O
MicroBooNE	–	CC [72]	Ar
MINERνA	CC [73–77]	CC [74,78,79], NC [80]	CH
MiniBooNE	CC [81,82]	CC [83], NC [84,85]	CH_2
MINOS	–	NC [86]	Fe
NOMAD	–	NC [87]	C
NOvA	–	NC [88]	C
SciBooNE	CC [89]	NC [90,91]	CH
T2K	CC [92,93]	–	CH, H_2O
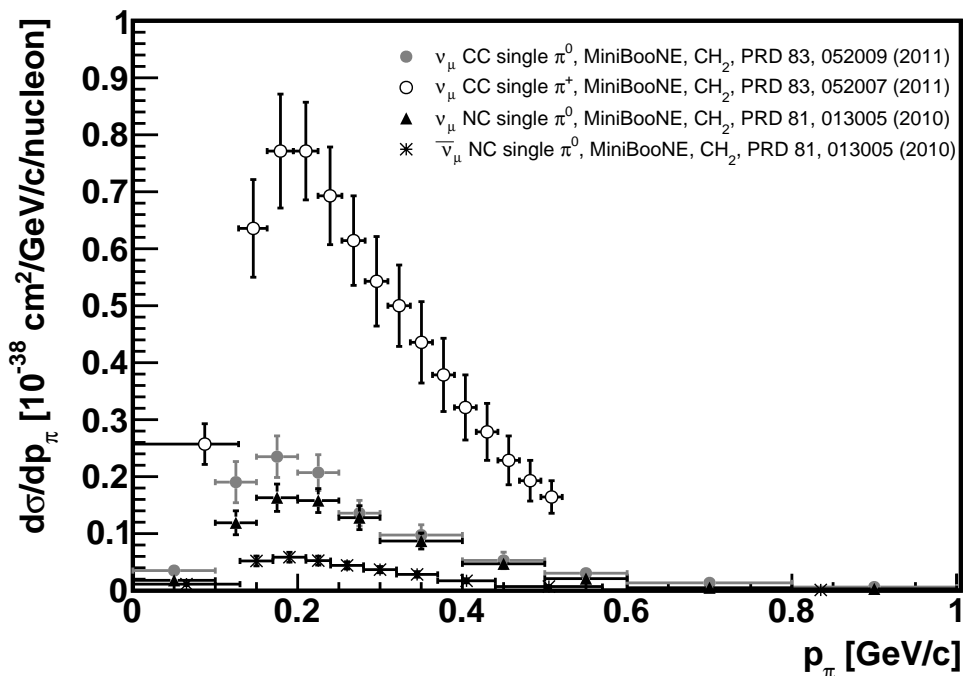
Figure 51.2: Differential cross sections for CC and NC pion production from MiniBooNE at a mean neutrino energy of 0.8 GeV. Shown here are the measurements as a function of the momentum of the outgoing pion in the interaction, a kinematic that is particularly sensitive to final state interactions. Other distributions are also available in the publications listed in the legend.

entire nucleus and produce a distinctly forward-scattered single pion final state. Both CC ($\nu_\mu A \to \mu^- A \pi^+$, $\overline{\nu}_\mu A \to \mu^+ A \pi^-$) and NC ($\nu_\mu A \to \nu_\mu A \pi^0, \overline{\nu}_\mu A \to \overline{\nu}_\mu A \pi^0$) processes are possible in this case. Even though the level of coherent pion production is small compared to their resonant counterpart, observations exist across a broad energy range and on multiple nuclear targets [94]. More recently, several modern neutrino experiments have either measured or set limits on coherent

pion production cross sections including ArgoNeuT [66], K2K [69], MINERvA [75,77], MiniBooNE [85], MINOS [86], NOMAD [87], NOvA [88], SciBooNE [89,91], and T2K [69].
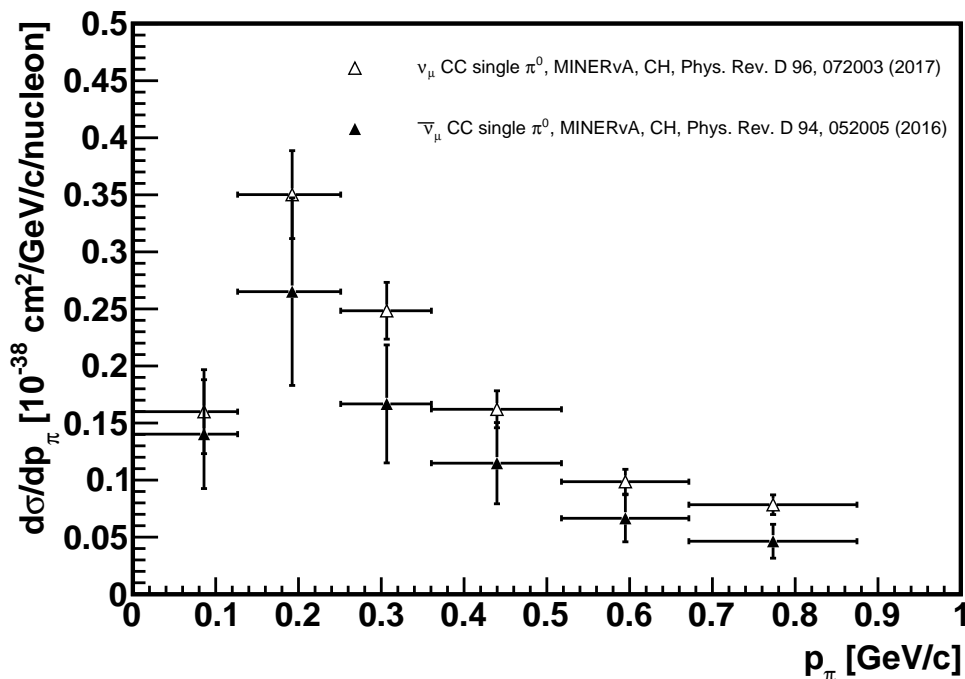

Figure 51.3: Differential cross sections for neutrino (W< 1.4 GeV) and antineutrino (W< 1.8 GeV) CC π^0 production from MINERvA at a mean neutrino energy of 3.3 GeV. Shown here are the measurements as a function of the momentum of the outgoing pion in the interaction, a kinematic that is particularly sensitive to final state interactions. Other distributions are available in the publications listed in the legend as well as for charged pion production [74].

As with QE scattering, a new appreciation for the significance of nuclear effects has surfaced in pion production channels, again due to the use of heavy nuclear targets in modern neutrino experiments. Many experiments have been careful to report cross sections for various detected final states, thereby not correcting for large and uncertain nuclear effects (e.g., pion rescattering, charge exchange, and absorption) which can introduce significant sources of uncertainty and model dependence. Providing the most comprehensive survey of neutrino single-pion production to date, MiniBooNE has published a total of 16 single- and double-differential cross sections for both the final state muon (in the case of CC scattering) and pions in these interactions; thus, providing the first measurements of these distributions (Fig. 51.2) [81–84]. MINERvA has recently produced similar kinematic measurements at higher neutrino energies (Fig. 51.3) [74, 76, 79] and T2K at lower energies [92]. Importantly, MINERvA has been working towards an improved nuclear model that can describe all of the pion reaction channels simultaneously, an issue that many experiments have struggled with up until now [74]. ArgoNeuT [67] and MicroBooNE [72] have been adding new information on single pion production in argon. Regardless of the interaction channel or target material, differential cross section measurements in terms of observed final state particle kinematics are preferred for their reduced model dependence and for the additional kinematic information they provide. Such a new direction has been the focus of modern measurements as opposed to the reporting of more model-dependent, historical cross sections as a function of E_ν

or Q^2. Together with similar results for other interaction channels, a better understanding and modeling of nuclear effects will be possible moving forward. MINERvA [95] has already taken a large step in this direction by explicitly tuning the physics in existing neutrino event generators to best fit the experimental data on pion production.

It should be noted that baryonic resonances can also decay to multi-pion, other mesonic (K, η, ρ, etc.), and even photon final states. Experimental results for these channels are typically sparse or non-existent [2]; however, photon production processes can be an important background for $\nu_\mu \to \nu_e$ appearance searches and thus have become the focus of recent experimental investigations, most notably in NOMAD [96] and T2K [97]. There have also been several recent measurements of kaon final states produced in neutrino NC and CC scattering in MINERvA [98–100] that are providing needed background constraints for certain nucleon decay searches.

51.4 Outlook

Currently operating experiments will continue to produce additional neutrino cross section measurements as they accumulate additional statistics, while a few new experiments will soon be coming online. Analysis of a broad energy range of data from MINERvA is providing some of the most detailed analysis of nuclear effects in neutrino interactions by examining multiple nuclei in a single experiment. Data from ArgoNeuT, ICARUS, MicroBooNE, and SBND will probe deeper into complex neutrino final states using the superior capabilities of liquid argon time projection chambers, while the T2K and NOvA near detectors will continue to collect high statistics samples in intense neutrino beams. Together with dedicated discussions between the experiments on how best to report neutrino cross section measurements [101] and accompanying improvements in nuclear model calculations [3], these investigations are crucial for significantly advancing our understanding of neutrino-nucleus scattering.

51.5 Acknowledgments

References

  [1] O. Benhar *et al.*, Phys. Rept. **700**, 1 (2017), [arXiv:1501.06448].

  [2] J. A. Formaggio and G. P. Zeller, Rev. Mod. Phys. **84**, 1307 (2012), [arXiv:1305.7513].

  [3] L. Alvarez-Ruso *et al.*, Prog. Part. Nucl. Phys. **100**, 1 (2018), [arXiv:1706.03621].

  [4] M. Tzanov *et al.* (NuTeV), Phys. Rev. **D74**, 012008 (2006), [hep-ex/0509010].

  [5] C. Anderson *et al.* (ArgoNeuT), Phys. Rev. Lett. **108**, 161802 (2012), [arXiv:1111.0103].

  [6] R. Acciarri *et al.* (ArgoNeuT), Phys. Rev. **D89**, 11, 112003 (2014), [arXiv:1404.4809].

  [7] P. Abratenko *et al.* (MicroBooNE), Phys. Rev. Lett. **123**, 13, 131801 (2019), [arXiv:1905.09694].

  [8] P. A. Rodrigues *et al.* (MINERvA), Phys. Rev. Lett. **116**, 071802 (2016), [Addendum: Phys. Rev. Lett.121,no.20,209902(2018)], [arXiv:1511.05944].

  [9] K. Abe *et al.* (T2K), Phys. Rev. **D87**, 9, 092003 (2013), [arXiv:1302.4908].

[10] K. Abe *et al.* (T2K), Phys. Rev. **D98**, 012004 (2018), [arXiv:1801.05148].

[11] C. Adams *et al.* (MicroBooNE), Eur. Phys. J. **C79**, 3, 248 (2019), [arXiv:1805.06887].

[12] K. Abe *et al.* (T2K) (2019), [arXiv:1904.09611].

[13] K. Abe *et al.* (T2K), Phys. Rev. **D96**, 5, 052001 (2017), [arXiv:1706.04257].

[14] B. G. Tice *et al.* (MINERvA), Phys. Rev. Lett. **112**, 23, 231801 (2014), [arXiv:1403.2103].

[15] J. Mousseau *et al.* (MINERvA), Phys. Rev. **D93**, 7, 071101 (2016), [arXiv:1601.06313].

[16] A. Kayis-Topaksu *et al.* (CHORUS), Nucl. Phys. **B798**, 1 (2008), [arXiv:0804.1869].

[17] O. Samoylov *et al.* (NOMAD), Nucl. Phys. **B876**, 339 (2013), [arXiv:1308.4750].

[18] D. Mason *et al.* (NuTeV), Phys. Rev. Lett. **99**, 192001 (2007).

[19] J. Devan *et al.* (MINERvA), Phys. Rev. **D94**, 11, 112007 (2016), [arXiv:1610.04746].

[20] L. Ren *et al.* (MINERvA), Phys. Rev. **D95**, 7, 072009 (2017), [Addendum: Phys. Rev.D97,no.1,019902(2018)], [arXiv:1701.04857].

[21] P. Adamson *et al.* (MINOS), Phys. Rev. **D81**, 072002 (2010), [arXiv:0910.2201].

[22] Q. Wu *et al.* (NOMAD), Phys. Lett. **B660**, 19 (2008), [arXiv:0711.1183].

[23] Y. Nakajima *et al.* (SciBooNE), Phys. Rev. **D83**, 012005 (2011), [arXiv:1011.2131].

[24] K. Abe *et al.* (T2K), Phys. Rev. **D90**, 5, 052010 (2014), [arXiv:1407.4256].

[25] K. Abe *et al.* (T2K), Phys. Rev. **D93**, 7, 072002 (2016), [arXiv:1509.06940].

[26] K. Abe *et al.* (T2K), Phys. Rev. Lett. **113**, 24, 241803 (2014), [arXiv:1407.7389].

[27] K. Abe *et al.* (T2K), Phys. Rev. **D91**, 112010 (2015), [arXiv:1503.08815].

[28] D. Ruterbories *et al.* (MINERvA), Phys. Rev. **D99**, 1, 012004 (2019), [arXiv:1811.02774].

[29] C. E. Patrick *et al.* (MINERvA), Phys. Rev. **D97**, 5, 052002 (2018), [arXiv:1801.01197].

[30] X. G. Lu *et al.* (MINERvA), Phys. Rev. Lett. **121**, 2, 022504 (2018), [arXiv:1805.05486].

[31] A. A. Aguilar-Arevalo *et al.* (MiniBooNE), Phys. Rev. **D81**, 092005 (2010), [arXiv:1002.2680].

[32] A. A. Aguilar-Arevalo *et al.* (MiniBooNE), Phys. Rev. **D88**, 3, 032001 (2013), [arXiv:1301.7067].

[33] K. Abe *et al.* (T2K), Phys. Rev. **D93**, 11, 112012 (2016), [arXiv:1602.03652].

[34] K. Abe *et al.* (T2K), Phys. Rev. **D97**, 1, 012001 (2018), [arXiv:1708.06771].

[35] K. Abe *et al.* (2019), [arXiv:1908.10249].

[36] K. Abe *et al.* (T2K), Phys. Rev. **D98**, 3, 032003 (2018), [arXiv:1802.05078].

[37] K. Mahn, C. Marshall and C. Wilkinson, Ann. Rev. Nucl. Part. Sci. **68**, 105 (2018), [arXiv:1803.08848].

[38] R. Acciarri *et al.* (ArgoNeuT), Phys. Rev. **D90**, 1, 012008 (2014), [arXiv:1405.4261].

[39] R. Gran *et al.* (K2K), Phys. Rev. **D74**, 052002 (2006), [hep-ex/0603034].

[40] G. A. Fiorentini *et al.* (MINERvA), Phys. Rev. Lett. **111**, 022502 (2013), [arXiv:1305.2243].

[41] L. Fields *et al.* (MINERvA), Phys. Rev. Lett. **111**, 2, 022501 (2013), [arXiv:1305.2234].

[42] M. Betancourt *et al.* (MINERvA), Phys. Rev. Lett. **119**, 8, 082001 (2017), [arXiv:1705.03791].

[43] T. Walton *et al.* (MINERvA), Phys. Rev. **D91**, 7, 071301 (2015), [arXiv:1409.4497].

[44] J. Wolcott *et al.* (MINERvA), Phys. Rev. Lett. **116**, 8, 081802 (2016), [arXiv:1509.05729].

[45] R. Gran *et al.* (MINERvA), Phys. Rev. Lett. **120**, 22, 221805 (2018), [arXiv:1803.09377].

[46] A. A. Aguilar-Arevalo *et al.* (MiniBooNE), Phys. Rev. Lett. **100**, 032301 (2008), [arXiv:0706.0926].

[47] A. A. Aguilar-Arevalo *et al.* (MiniBooNE), Phys. Rev. **D82**, 092005 (2010), [arXiv:1007.4730].

[48] A. A. Aguilar-Arevalo *et al.* (MiniBooNE), Phys. Rev. **D91**, 1, 012004 (2015), [arXiv:1309.7257].

[49] P. Adamson *et al.* (MINOS), Phys. Rev. **D91**, 1, 012005 (2015), [arXiv:1410.8613].

[50] V. Lyubushkin *et al.* (NOMAD), Eur. Phys. J. **C63**, 355 (2009), [arXiv:0812.4543].

[51] L. Wan *et al.* (Super-Kamiokande), Phys. Rev. **D99**, 3, 032005 (2019), [arXiv:1901.05281].

[52] K. Abe *et al.* (T2K), Phys. Rev. **D91**, 11, 112002 (2015), [arXiv:1503.07452].

[53] K. Abe *et al.* (T2K), Phys. Rev. **D92**, 11, 112003 (2015), [arXiv:1411.6264].

[54] K. Abe *et al.* (T2K), Phys. Rev. **D90**, 7, 072012 (2014), [arXiv:1403.3140].

[55] J. Carlson *et al.*, Phys. Rev. **C65**, 024002 (2002), [arXiv:nucl-th/0106047].

[56] H. Gallagher, G. Garvey and G. P. Zeller, Ann. Rev. Nucl. Part. Sci. **61**, 355 (2011).

[57] G. T. Garvey *et al.*, Phys. Rept. **580**, 1 (2015), [arXiv:1412.4294].

[58] O. Palamara (ArgoNeuT), JPS Conf. Proc. **12**, 010017 (2016).

[59] M. Elkins *et al.* (MINERvA), Phys. Rev. **D100**, 5, 052002 (2019), [arXiv:1901.04892].

[60] L. A. Ahrens *et al.*, Phys. Rev. **D35**, 785 (1987).

[61] J. Brunner *et al.* (SKAT), Z. Phys. **C45**, 551 (1990).

[62] V. V. Ammosov *et al.*, Z. Phys. **C36**, 377 (1987); O. Erriquez *et al.*, Phys. Lett. **70B**, 383 (1977); T. Eichten *et al.*, Phys. Lett. **40B**, 593 (1972).

[63] C. Wilkinson *et al.*, Phys. Rev. **D90**, 11, 112017 (2014), [arXiv:1411.4482].

[64] A. S. Meyer *et al.*, Phys. Rev. **D93**, 11, 113015 (2016), [arXiv:1603.03048].

[65] P. Rodrigues, C. Wilkinson and K. McFarland, Eur. Phys. J. **C76**, 8, 474 (2016), [arXiv:1601.01888].

[66] R. Acciarri *et al.* (ArgoNeuT), Phys. Rev. Lett. **113**, 26, 261801 (2014), [erratum: Phys. Rev. Lett.114,no.3,039901(2015)], [arXiv:1408.0598].

[67] R. Acciarri *et al.* (ArgoNeuT), Phys. Rev. **D96**, 1, 012006 (2017), [arXiv:1511.00941].

[68] A. Rodriguez *et al.* (K2K), Phys. Rev. **D78**, 032003 (2008), [arXiv:0805.0186].

[69] M. Hasegawa *et al.* (K2K), Phys. Rev. Lett. **95**, 252301 (2005), [hep-ex/0506008].

[70] C. Mariani *et al.* (K2K), Phys. Rev. **D83**, 054023 (2011), [arXiv:1012.1794].

[71] S. Nakayama *et al.* (K2K), Phys. Lett. **B619**, 255 (2005), [hep-ex/0408134].

[72] C. Adams *et al.* (MicroBooNE), Phys. Rev. **D99**, 9, 091102 (2019), [arXiv:1811.02700].

[73] B. Eberly *et al.* (MINERvA), Phys. Rev. **D92**, 9, 092008 (2015), [arXiv:1406.6415].

[74] C. L. McGivern *et al.* (MINERvA), Phys. Rev. **D94**, 5, 052005 (2016), [arXiv:1606.07127].

[75] A. Higuera *et al.* (MINERvA), Phys. Rev. Lett. **113**, 26, 261802 (2014), [arXiv:1409.3835].

[76] T. Le *et al.* (MINERvA), Phys. Rev. **D100**, 5, 052008 (2019), [arXiv:1906.08300].

[77] A. Mislivec *et al.* (MINERvA), Phys. Rev. **D97**, 3, 032014 (2018), [arXiv:1711.01178].

[78] T. Le *et al.* (MINERvA), Phys. Lett. **B749**, 130 (2015), [arXiv:1503.02107].

[79] O. Altinok *et al.* (MINERvA), Phys. Rev. **D96**, 7, 072003 (2017), [arXiv:1708.03723].

[80] J. Wolcott *et al.* (MINERvA), Phys. Rev. Lett. **117**, 11, 111801 (2016), [arXiv:1604.01728].

[81] A. A. Aguilar-Arevalo *et al.* (MiniBooNE), Phys. Rev. **D83**, 052007 (2011), [arXiv:1011.3572].

[82] A. A. Aguilar-Arevalo *et al.* (MiniBooNE), Phys. Rev. Lett. **103**, 081801 (2009), [arXiv:0904.3159].

[83] A. A. Aguilar-Arevalo *et al.* (MiniBooNE), Phys. Rev. **D83**, 052009 (2011), [arXiv:1010.3264].

[84] A. A. Aguilar-Arevalo *et al.* (MiniBooNE), Phys. Rev. **D81**, 013005 (2010), [arXiv:0911.2063].

[85] A. A. Aguilar-Arevalo *et al.* (MiniBooNE), Phys. Lett. **B664**, 41 (2008), [arXiv:0803.3423].

[86] P. Adamson *et al.* (MINOS), Phys. Rev. **D94**, 7, 072006 (2016), [arXiv:1608.05702].

[87] C. T. Kullenberg *et al.* (NOMAD), Phys. Lett. **B682**, 177 (2009), [arXiv:0910.0062].

[88] M. A. Acero *et al.* (NOvA) (2019), [arXiv:1902.00558].

[89] K. Hiraide *et al.* (SciBooNE), Phys. Rev. **D78**, 112004 (2008), [arXiv:0811.0369].

[90] Y. Kurimoto *et al.* (SciBooNE), Phys. Rev. **D81**, 033004 (2010), [arXiv:0910.5768].

[91] Y. Kurimoto *et al.* (SciBooNE), Phys. Rev. **D81**, 111102 (2010), [arXiv:1005.0059].

[92] K. Abe *et al.* (T2K), Phys. Rev. **D95**, 1, 012010 (2017), [arXiv:1605.07964].

[93] K. Abe *et al.* (T2K), Phys. Rev. Lett. **117**, 19, 192501 (2016), [arXiv:1604.04406].

[94] P. Vilain *et al.* (CHARM-II), Phys. Lett. **B313**, 267 (1993); A compilation of historical coherent pion production data.

[95] P. Stowell *et al.* (MINERvA), Phys. Rev. **D100**, 7, 072005 (2019), [arXiv:1903.01558].

[96] C. T. Kullenberg *et al.* (NOMAD), Phys. Lett. **B706**, 268 (2012), [arXiv:1111.3713].

[97] K. Abe *et al.* (T2K), J. Phys. **G46**, 8, 08LT01 (2019), [arXiv:1902.03848].

[98] C. M. Marshall *et al.* (MINERvA), Phys. Rev. **D94**, 1, 012002 (2016), [arXiv:1604.03920].

[99] C. M. Marshall *et al.* (MINERvA), Phys. Rev. Lett. **119**, 1, 011802 (2017), [arXiv:1611.02224].

[100] Z. Wang *et al.* (MINERvA), Phys. Rev. Lett. **117**, 6, 061802 (2016), [arXiv:1606.08890].

[101] M. Betancourt *et al.*, Phys. Rept. **773-774**, 1 (2018), [arXiv:1805.07378].